

ORIGINAL ARTICLE

CMHX008, a PPAR γ partial agonist, enhances insulin sensitivity with minor influences on bone loss

Yi Hou ^{a,c}, Xuemei Cao ^{a,c}, Xiangnan Hu ^b, Xinyu Li ^a,
Xiaoqin Shi ^{a,c}, Hongying Wang ^{a,c}, Chuan Peng ^{a,c}, Jiayu Li ^{a,c},
Jibin Li ^d, Qifu Li ^c, Chaodong Wu ^f, Xiaoqiu Xiao ^{a,c,e,*}

^a Department of Endocrinology, The First Affiliated Hospital of Chongqing Medical University, Chongqing, 400016, China

^b College of Pharmacy, Chongqing Medical University, China

^c The Chongqing Key Laboratory of Translational Medicine in Major Metabolic Diseases, The First Affiliated Hospital of Chongqing Medical University, Chongqing, 400016, China

^d Department of Nutrition and Food Hygiene, School of Public Health and Management, Chongqing Medical University, Chongqing, 400016, China

^e Canada-China-New Zealand Joint Laboratory of Maternal and Fetal Medicine, Chongqing Medical University, Chongqing, 400016, China

^f Department of Nutrition and Food Science, Texas A&M University, College Station, TX, 77843, USA

Received 27 April 2018; accepted 31 May 2018

Available online 6 June 2018

KEYWORDS

Osteoblasts;
Peroxisome
proliferator-activated
receptor γ ;
Thiazolidinediones;
TR-FRET;
Type 2 diabetes
mellitus

Abstract Traditional thiazolidinediones (TZDs), such as rosiglitazone, are peroxisome proliferator-activated receptor γ (PPAR γ) potent agonists that can be used to treat type 2 diabetes but carry unwanted effects, including increased risk for fracture. The present work aimed to compare the insulin-sensitizing efficacies and bone-loss side effects of CMHX008, a novel TZDs-like PPAR γ partial agonist, with those of rosiglitazone. A TR-FRET PPAR γ competitive binding assay was used to compare the binding affinity between CMHX008 and rosiglitazone. Mice were administered vehicle, CMHX008 or rosiglitazone for 16 weeks. Mesenchymal stem cells (MSCs) were used to examine differences in differentiation into osteoblasts after compounds treatment. TR-FRET showed lower affinity to PPAR γ by CMHX008 compared with rosiglitazone. Mice treated with CMHX008 showed insulin sensitization similar to that of mice treated with rosiglitazone, which was related to the significant inhibition of PPAR γ Ser273 phosphorylation and improved insulin sensitivity by facilitating the phosphorylation of insulin receptor and Akt in adipose tissues. Micro-CT and histomorphometric analyses demonstrated

* Corresponding author. Department of Endocrinology, The First Affiliated Hospital of Chongqing Medical University, Chongqing, 400016, China.

E-mail address: bshaw2001@163.com (X. Xiao).

Peer review under responsibility of Chongqing Medical University.

that the degree of trabecular bone loss after treatment with CMHX008 was weaker than that observed with rosiglitazone, as evidenced by consistent changes in BV/TV, Tb.N, Tb.Th, Tb.Sp, and the mineral apposition rate. MSCs treated with CMHX008 showed higher ALP activity and mRNA levels of bone formation markers than did cells treated with rosiglitazone in the osteoblast differentiation test. Thus, CMHX008 showed insulin-sensitizing effects similar to those of rosiglitazone with a lower risk of bone loss, suggesting that PPAR γ sparing eliminates the skeletal side effects of TZDs while maintaining their insulin-sensitizing properties.

Copyright © 2018, Chongqing Medical University. Production and hosting by Elsevier B.V. This is an open access article under the CC BY-NC-ND license (<http://creativecommons.org/licenses/by-nc-nd/4.0/>).

Introduction

Type 2 diabetes mellitus (T2DM) has become a global epidemic metabolic disease over the last several decades.^{1,2} One important characteristic of T2DM is resistance to insulin or reduced insulin secretion. Thiazolidinediones (TZDs) improve whole-body insulin sensitivity and reduce the blood glucose levels in patients with T2DM as an activator of peroxisome proliferator-activated receptor γ (PPAR γ).³ However, there are great concerns about classical TZDs, such as rosiglitazone, due to their risk of fluid retention, weight gain, bone loss and congestive heart failure.^{4,5} A recent safety evaluation demonstrated that rosiglitazone showed no increased risk of heart attack compared to the standard T2DM medicines metformin and sulfonylurea.⁶ Another critical review performed on TZDs in the treatment of T2DM considered that TZDs should appropriately continue use after evaluating the positive and adverse effects.⁷

Bone loss and skeletal fragility, especially in female patients, are common undesirable effects after the long-term usage of classical TZDs.^{8–10} Physiologically, bone is constantly remodeled with bone resorption by osteoclasts, followed by bone formation by osteoblasts, depending on the subtle coordination between these two types of cells. Osteoblasts originate from mesenchymal progenitors, while osteoclast cells arise from hematopoietic progenitors of the monocyte/macrophage lineage. The concerted coupling of bone resorption and formation are accurately controlled by a variety of neuronal and hormonal factors, including nuclear receptor signaling.¹¹ PPAR γ is a nuclear receptor that is highly expressed in white and brown adipose tissue (WAT and BAT), which plays an essential role in adipocyte differentiation, glucose homeostasis and inflammation,^{12,13} and also regulates the bone remodeling by increasing the abundance of osteoblasts without affection neither the differentiation nor the function of osteoclasts.¹⁴ Although PPAR γ activators have been demonstrated as effective in the treatment of T2DM, other evidence also showed that modulating or even inhibiting PPAR γ activity might be the preferred therapeutic strategy to improve glucose homeostasis while preventing adipogenesis.^{15–17} The attainment of insulin sensitizing properties does not require maximal PPAR γ activation, which is one of the reasons why full and weak PPAR γ agonists may provide comparable insulin sensitization and rationale to design partial PPAR γ agonists.¹⁸ High-fat-diet-fed obese mice exhibit activated

cyclin-dependent protein kinase-5 (CDK5) within adipose tissues, and rosiglitazone blocks the CDK5-mediated phosphorylation of PPAR γ at serine 273.¹⁹ Selective PPAR γ modulators (SPPARMs), due to their PPAR γ partial agonistic behavior, improve glucose homeostasis but present few of the aforementioned side effects.^{18,20–22} These studies provide insight into the mechanism underlying PPAR γ -mediated insulin sensitization and its associated side effects and provide a potential strategy to develop safer PPAR γ -specific drugs that reduce the adverse effects associated with TZDs while preserving insulin-sensitizing potential.

We recently identified CMHX008, a TZDs analog, chemically known as 3-tert-butoxycarbonylmethyl-5-[4-[2-[N-methyl-N-(2-pyridyl)amino]-ethoxy]benzyl]thiazolidine-2,4-dione (Fig. 1A), as a PPAR γ partial agonist with a hypoglycemic effect comparable to that of rosiglitazone but with lower adipogenic capacity.²³ To further characterize the pharmacological features of CMHX008, we performed a time-resolved fluorescence resonance energy transfer (TR-FRET) assay to determine the competitive binding affinity

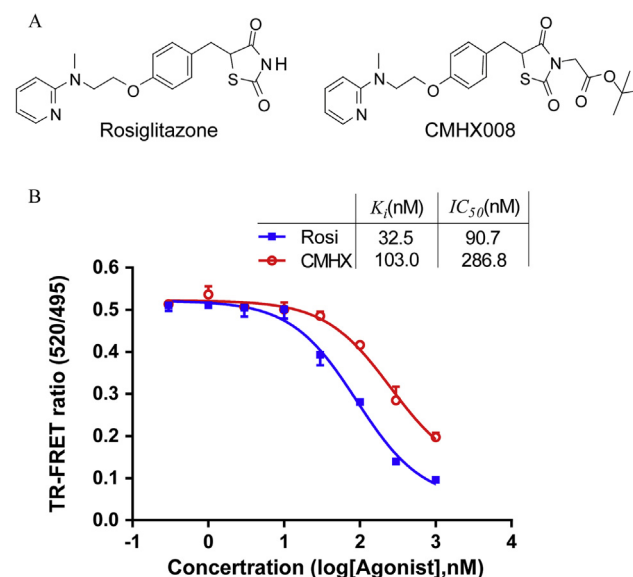


Figure 1 The binding affinity of rosiglitazone (Rosi) and CMHX008 (CMHX) on PPAR γ . (A) Chemical structure of Rosi and CMHX. (B) TR-FRET competitive binding assay was used to examine the binding affinity of the human PPAR γ in response to rosiglitazone or CMHX008 at concentrations ranging from 0.3 to 1000 nM ($n = 3$).

of CMHX008 with PPAR γ compared to that with rosiglitazone. The therapeutic and side effects, especially on bone mineral metabolism, were evaluated in mice after relatively long (16 weeks) treatment. Furthermore, differences in differentiation into osteoblasts from mesenchymal stem cells (MSCs) after treatment with CMHX008 and rosiglitazone were investigated.

Materials and methods

Animals and diets

All experimental procedures were approved by the Institutional Animal Care and Use Committee of Chongqing Medical University. Male C57BL/6 mice (6 weeks old) were obtained from the Animal Laboratory of Chongqing Medical University. Leptin defect *ob/ob* mice were generated through breeding heterozygous *ob* \pm littermates. All mice were housed under standard conditions with a 12 h/12 h light-dark cycle and constant temperature. C57BL/6 mice were fed either a low-fat diet (LFD, D12450B, 10% Kcal from fat, Research Diets, New Brunswick, USA) or high-fat diet (HFD, D12492, 60% Kcal from fat, Research Diets, New Brunswick, USA). After 12 weeks, HFD-fed mice with a body weight higher than the average plus 3 standard deviations of the LFD mice were considered diet-induced obese mice.⁶ HFD fed obese mice were randomly separated into seven groups: CMHX008 1 mg/kg ($n = 7$), 3 mg/kg ($n = 7$) or 10 mg/kg ($n = 13$), rosiglitazone (Taiji Group Ltd, Chongqing, China) 1 mg/kg ($n = 7$), 3 mg/kg ($n = 7$) or 10 mg/kg ($n = 13$), and vehicle ($n = 13$). The chemicals and vehicle were administered once daily by intragastric gavage for an additional 16 weeks. LFD and *ob/ob* mice were treated with 10 mg/kg/day of CMHX008 or rosiglitazone (LFD, $n = 8$ /group; *ob/ob*, $n = 4$ –6/group). At the end of the study, all mice were euthanatized by CO₂ inhalation and sacrificed in a non-fasting state. Trunk blood, epididymal white adipose tissues (WAT), tibia, femur, and other tissues were collected.

PPAR γ competitive ligand binding analysis

Serial concentrations of compounds were incubated with GST-fused human PPAR γ -LBD, terbium-labeled anti-GST antibody, and PPAR ligand within TR-FRET PPAR γ Competitive Binding Assay Kit (A15144, Invitrogen, Carlsbad, USA) in the dark at room temperature. The FRET signal was measured by excitation at 340 nm and emission at 520 nm for fluorescein and 495 nm for terbium. The signal may decrease when the test compounds binding to PPAR γ -LBD competed with and replaced Pan-PPAR Green. The binding to the PPAR γ -LBD was analyzed by the 520 nm/495 nm ratio.

Intraperitoneal glucose tolerance test (iGTT)

Intraperitoneal glucose tolerance test (iGTT) was performed 10 weeks after compounds or vehicle treatment. Mice were fasted for 12 h with free access to water, 2 g/kg of glucose was intraperitoneally injected and blood glucose was measured at 0, 15, 30, 60, 120 min after injection.²⁴

Indirect calorimetry analysis

Mice were individually housed in metabolic chambers (TSE PhenoMaster/LabMaster Systems, Berlin, Germany) to acclimate for 4 d before indirect calorimetry studies. The system was used to measure the oxygen consumption (VO₂), carbon dioxide production (VCO₂), ambulatory activity, and food intake of the individual mice, as previously described.²⁵ Data were collected and averaged from 3-day tests.

RNA isolation and quantitative real-time RT-PCR analysis

Total RNAs were isolated and purified using the Total RNA Extraction Kit (RP1202, Biotek, Beijing, China). One milligram of total RNA was reverse transcribed on Thermal Cycler (Veriti, Applied Biosystems, Singapore). Real-time PCR was performed using SYBR and gene-specific primers and quantitated on the RT-qPCR detection system (CFX96, BIO-RAD, Singapore). All reactions were performed in triplicate, and relative mRNA levels were calculated by the comparative threshold cycle method by using GAPDH as an internal control. The primer sequences are provided as follows: Gapdh (forward – GACATCAAGAAGGTGGTGAAGC; reverse – GAAGGTGAAGAGTGGGAGTT); osteocalcin (Ocn) (forward – CAAGCAGGGTTAAGCTCACA; reverse – GGTA GTGAACAGACTCCGGC); Runx2 (forward – GAAGCUUGAUGACUCUAAATTA; reverse – UUUAGAGUCAUCAAGCUUCTC).

Western blotting analysis

WAT or cells were homogenized in buffer with protease and phosphatase inhibitors. Total protein was extracted with TRIzol Reagent (Sigma). Protein content was determined with a protein assay kit, and samples were then aliquoted and stored at –80 °C. The protein was separated by SDS-PAGE and transferred to nitrocellulose membranes, followed by blocking for 2 h and incubation for 12 h at 4 °C with primary antibodies. Anti-Insulin Receptor β (#3025), anti-Phospho-insulin receptor β (#3024), Phospho-Akt (Ser473) (#4060), and anti-Akt (#4691) antibodies were obtained from Cell Signaling Technology (Danvers, Massachusetts, USA); anti-phospho-PPAR γ (ser273) (bs-4888R) was purchased from Bioss Inc. (Woburn, MA, USA); and anti-PPAR gamma (ab59256), anti-Osteocalcin (ab93876) and anti-Runx2 (ab23981) were obtained from Abcam (Cambridge, UK). The membrane was then incubated with the secondary antibodies for 1 h at room temperature. The protein bands were visualized with an enhanced chemiluminescence (ECL) detection system. The band intensity was quantified with Fusion FX (Vliber Lourmat, Australia) software and all quantitative analyses were normalized to β -actin or GAPDH.

Micro-computed tomography (μ CT) analysis

The right femur was measured by using a μ CT scanner (VivaCT 40, Scanco Medical AG, Switzerland) after the removal of soft tissues and overnight fixation in 4% paraformaldehyde. The bone trabecular morphometry of distal

metaphysis was performed at 100 kV and 98 μ A between frames. The two-dimensional images were used to generate three-dimensional reconstructions to obtain quantitative data with the 3D Creator software supplied with the instrument. One millimeter of trabecular bone (96 slices) was analyzed (Fig. 4A), beginning with an image at 1 mm from the epiphyseal line.

Histomorphometrical analysis of bone

Calcein (C0875, Sigma, USA) and alizarin red (A5533, Sigma, USA) were used in double labeling test to evaluate the bone mineral apposition rate (MAR). MAR, calculated as the interlabel width/labeling period, is indicative of the amount of newly formed mineralized osteoid per day. Briefly, calcein (20 mg/kg) and alizarin red (30 mg/kg) were subcutaneously injected in HFD mice treatment at a dose of

10 mg/kg/day at 14 and 4 days prior to sacrifice. After removing the soft tissues, the right femurs were fixed in 75% ethanol and embedded in methylmethacrylate. Longitudinal sections of 80 μ m thickness were cut by using a polycut-E microtome (LEICA1600, Germany) and ground to a final thickness of \sim 30 μ m, followed by imaging using a fluorescence microscope (FV1000, OLYMPUS, Japan).

Induction of osteoblastic differentiation

MSCs (C3H/10T1/2, ATCC, Manassas, VA, USA) were cultured in DMEM/F12 medium (HyClone, Utah, USA) containing 10% FBS (PAN, Adenbach, German). After growing to \sim 80% confluency, the cells were switched into osteoblast differentiation medium (DMEM/F12 plus 10 mM β -glycerophosphate, 50 μ g/ml ascorbic acid, 0.1 μ M dexamethasone).²⁶ The cells were treated with vehicle, rosiglitazone

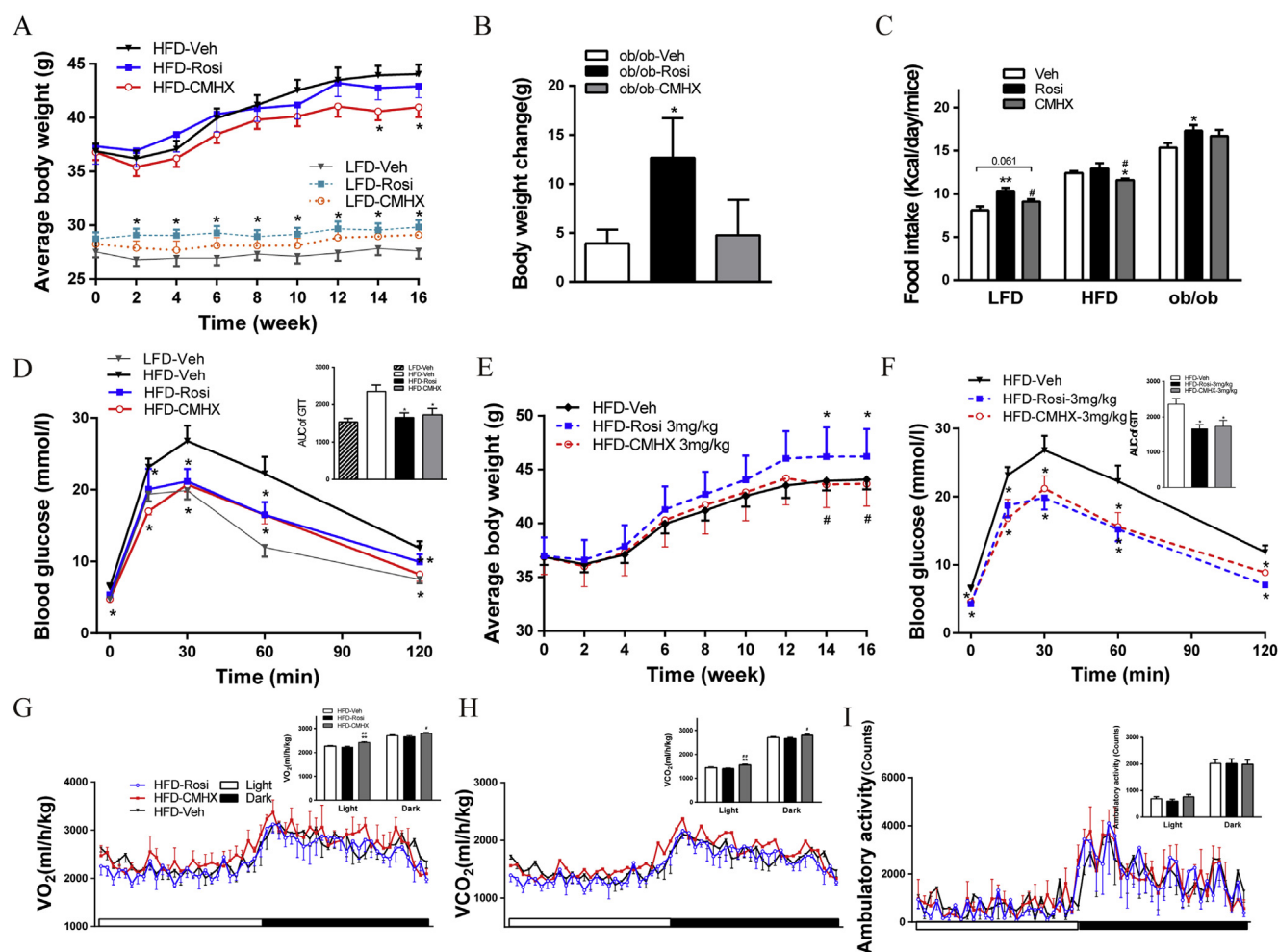


Figure 2 Effects of rosiglitazone (Rosi) or CMX008 (CMHX) on body weight (BW), food intake (FI), glucose homeostasis, and metabolic rate. (A) BW of HFD and LFD mice treated with 10 mg/kg/day of Rosi or CMHX for 16 weeks ($n = 10\text{--}13/\text{group}$). (B) BW changes in *ob/ob* mice treated with 10 mg/kg/day of Rosi or CMHX for 16 weeks ($n = 4\text{--}6/\text{group}$). (C) Daily FI of mice treated with 10 mg/kg/day measured two weeks before sacrifice ($n = 4\text{--}6/\text{group}$). (D) Glucose tolerance test (GTT) of HFD mice treated with 10 mg/kg/day performed at 10 weeks after treatment with the chemicals and area under the curve (AUC) of GTT ($n = 5\text{--}10/\text{group}$). (E) BW of HFD mice treated with 3 mg/kg/day of Rosi or CMHX for 16 weeks ($n = 5/\text{group}$). (F) GTT of HFD mice treated with 3 mg/kg/day performed at 10 weeks after treatment with the chemicals and AUC of GTT ($n = 7/\text{group}$). (G–I) Oxygen consumption (VO_2), carbon dioxide production (VCO_2) and ambulatory activity were measured for HFD mice treated with 10 mg/kg/day. * $P < 0.05$, ** $P < 0.01$, versus Veh, # $P < 0.05$, ## $P < 0.01$ versus Rosi.

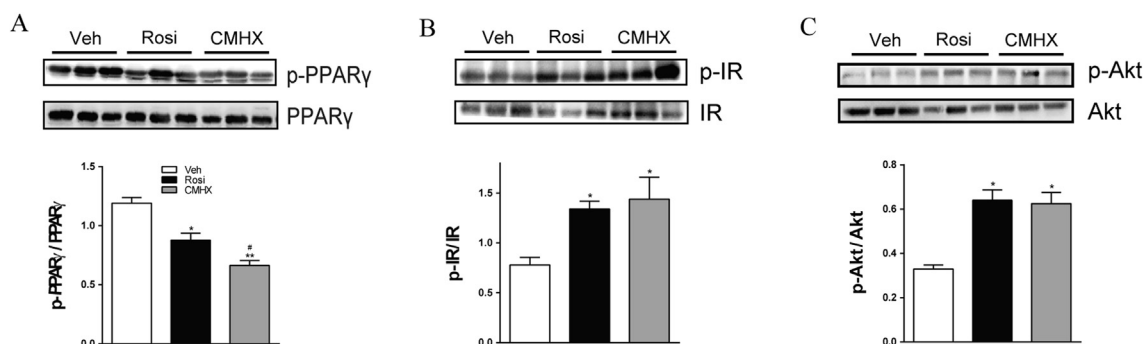


Figure 3 Effects of rosiglitazone (Rosi) or CMX008 (CMHX) treatment on phosphorylation of PPAR γ (p-PPAR γ), insulin receptor (p-IR) and Akt (p-Akt). Representative Western blots of protein phosphorylation (A, B, C) in white adipose tissue. Bar graphs show the p-PPAR γ , p-IR and p-Akt levels normalized to total appropriate protein levels. * $P < 0.05$, ** $P < 0.01$ versus Veh, # $P < 0.05$ versus Rosi ($n = 7$ /group).

(3 μ M), or CMX008 (3 μ M) at the start of differentiation. After differentiation for 7 days, the cell lysates were collected for western blotting. On day 14, alkaline phosphatase (ALP) staining was performed in mature osteoblasts and transcriptional levels of OCN and Runx2 were examined. The formation of mineralized matrix nodules was determined by alizarin red staining at day 21.

Staining and quantification for alkaline phosphatase and Alizarin red

Differentiated cells were rinsed and fixed. For ALP staining, fixed cells were stained with BCIP/NBT ALP staining solution (C3206, Beyotime, Beijing, China), and observed under Nikon microscope. For ALP quantification, differentiated cell lysates were homogenized on ice, and the supernatants were collected and mixed with ALP assay (P0321, Beyotime, Beijing, China), and ALP activity was determined by measuring absorbance at 405 nm. For Alizarin red staining (ARS), the fixed cells were stained with alizarin red (G8550, Solarbio, Beijing, China). The calcium deposition bounded with alizarin red was observed and photographed with a microscope. ARS quantification was performed by solubilizing the dye in cetylpyridinium chloride and the solution was detected at the absorbance of 570 nm.

Statistical analysis

IC₅₀ value was analyzed through nonlin fit of GraphPad Prism. Other data were presented as means \pm standard error of mean. The statistical significance of animal types and drug treatment effects was assessed by applying a one-way analysis of variance (ANOVA) in the SPSS 21 statistical package (SPSS Inc., USA). In all experiments, a value of $P < 0.05$ was considered significant.

Results

CMX008 was identified as a selective PPAR γ partial agonist

Our previous luciferase reporter assay and molecular docking studies indicated that CMX008 is a SPPARM.²³ To

further confirm the efficiency of CMX008 bound to PPAR γ , we performed a competitive TR-FRET ligand-binding assay. Fig. 1B shows that CMX008 directly bound to purified human PPAR γ -LBD with a half-inhibitory concentration (IC₅₀) of 286.8 nM (95% confidence intervals, 221.6–371.1 nM) and inhibition constant (K_i) of 103.0 nM. The IC₅₀ and K_i values for rosiglitazone were 90.7 nM (95% confidence intervals, 70.96–115.9 nM) and 32.5 nM, respectively, suggesting that CMX008 was weaker in binding to PPAR γ compared with rosiglitazone.

CMX008 treatment showed insulin sensitization comparable to that of rosiglitazone

The body weight of HFD mice treated with 10 mg/kg/day of CMX008 (HFD-CMX) was significantly reduced, while HFD mice treated with the same dose of rosiglitazone (HFD-Rosi) showed no significant difference compared with that of HFD mice treated with vehicle (HFD-Veh) (Fig. 2A). The body weight of HFD-Rosi mice treated at a dose of 3 mg/kg/day (HFD-Rosi-3 mg) (Fig. 2E) was significantly increased compared with HFD-Veh and HFD-CMX-3 mg mice, but no difference was observed at a dose of 1 mg/kg/day (data not shown). LFD mice treated with rosiglitazone (LFD-Rosi) showed increased body weights (Fig. 2A). The body weight change in *ob/ob* mice showed a significant increase after treatment with rosiglitazone (*ob/ob*-Rosi) compared with that after treatment with vehicle (*ob/ob*-Veh) (Fig. 2B). Accordingly, the food intake of LFD-Rosi or *ob/ob*-Rosi mice showed a significant increase or trend to increase compared with their vehicle-treated counterparts (Fig. 2C). HFD-CMX mice exhibited a significant reduction in food intake compared with HFD-Veh and HFD-Rosi mice at a dose of 10 mg/kg/day (Fig. 2C). Low dosage treatment showed no difference in food intake (data not shown). After intraperitoneal loading glucose, both HFD-CMX and HFD-Rosi mice showed a similar decrease in blood glucose levels at all tested time points compared with that of HFD-Veh (Fig. 2D). The same trend was found after treatment with a low dosage of 3 mg/kg/day (Fig. 2F). HFD-CMX mice showed higher VO₂ and VCO₂ during both light and dark phases of a 24-h monitoring period compared with

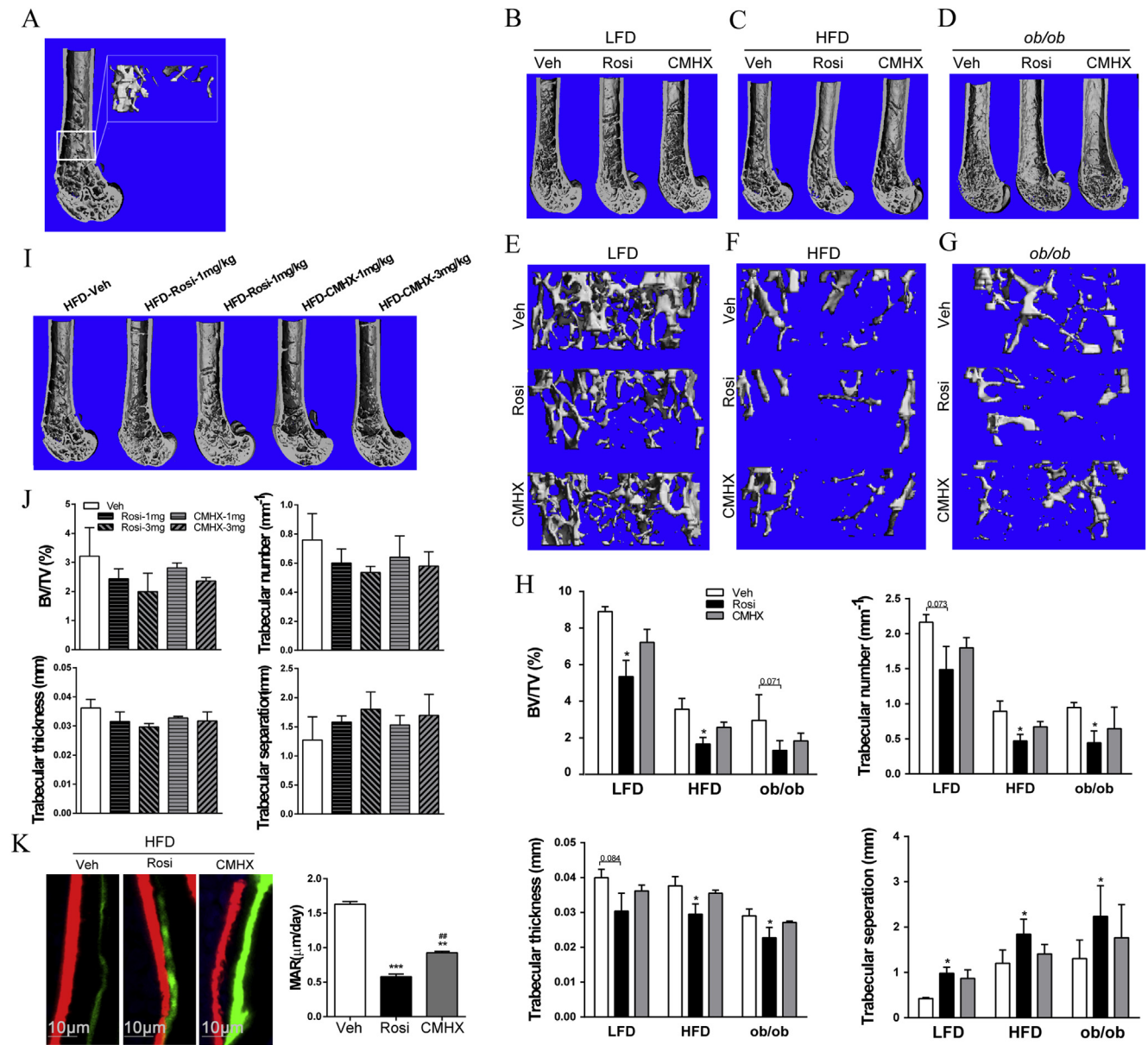


Figure 4 Effect of rosiglitazone (Rosi) or CMHX008 (CMHX) on bone formation. Mice were treated with vehicle (Veh), 1 mg/kg/day, 3 mg/kg/day or 10 mg/kg/day of rosiglitazone (Rosi) or CMHX008 (CMHX) for 16 weeks. (A) Three-dimensional μ CT images of the longitudinal section of the distal femur selected based on median value of bone volume/tissue volume (BV/TV), and the rectangle shows the location of trabecular bone. Representative μ CT images of longitudinal section of distal femur and trabecular bone from LFD (B and E), HFD (C and F) and *ob/ob* (D and G) mice treated with 10 mg/kg/day, respectively. The quantified μ CT images of BV/TV, trabecular number, trabecular thickness, and trabecular separation of LFD, HFD and *ob/ob* mice treated at 10 mg/kg/day (H) and HFD mice treated at 1 and 3 mg/kg/day (J). (I) Representative μ CT images of longitudinal section of distal femur of HFD mice treated at 1 and 3 mg/kg/day. (K) Representative mineral apposition rate (MAR) of HFD mice treated at 10 mg/kg/day. All data are expressed as the means \pm SEM. N = 6 per group in HFD mice and 4–5 per group in LFD and *ob/ob* mice. *P < 0.05, **P < 0.01, ***P < 0.001 versus Veh, ##P < 0.01 versus Rosi.

HFD-Veh and HFD-Rosi mice at a dose of 10 mg/kg/day, but there was no difference in ambulatory activity (Fig. 2G–I).

CMHX008 improves insulin sensitivity and inhibits PPAR γ phosphorylation in HFD mice

In WAT of HFD mice, the protein expression of PPAR γ phosphorylation (p-PPAR γ), total PPAR γ , insulin receptor β

phosphorylation (p-IR), total IR, Akt phosphorylation (p-Akt) and total Akt were measured by western blotting. The phosphorylation of PPAR γ at serine 273 stimulates the expression of adipose tissue genes related to insulin resistance and diabetes.^{19,27} As shown in Fig. 3A, at a dose of 10 mg/kg/day, both HFD-Rosi and HFD-CMHX mice displayed significantly inhibited PPAR γ phosphorylation, and HFD-CMHX mice showed stronger inhibition than that of HFD-Rosi mice. HFD mice treated with rosiglitazone or

CMHX008 showed increased protein levels of p-IR (Fig. 3B) and p-Akt (Fig. 3C).

CMHX008 treatment results in the minor bone loss

Micro-CT image of an undecalcified distal femur showed evidence of the overall loss of trabecular bone in HFD and *ob/ob* mice compared with that of LFD mice without any drug treatment. Treatment with either rosiglitazone or CMHX008 at the dose of 10 mg/kg/day in each type of mice displayed further loss of trabecular bone compared with vehicle treatment (Fig. 4B–D). The images of trabecular bone fragments further confirmed that rosiglitazone or CMHX008 treatment resulted in bone loss compared with vehicle treatment in LFD, HFD and *ob/ob* mice and, more importantly, that mice treated with rosiglitazone had a more severe decline than did mice treated with CMHX008 (Fig. 4E–G). Quantitative μ CT data of rosiglitazone-treated HFD mice indicated a significant decrease in the bone volume over tissue volume ratio (BV/TV), trabecular number (Tb.N) and trabecular thickness (Tb.Th) in the region of interest, which was consistent with the increase in trabecular separation (Tb.Sp), while CMHX008 treatment did not alter the above skeletal markers (Fig. 4H). A similar change was also observed in LFD and *ob/ob* mice, although some trabecular bone parameters of LFD and *ob/ob* mice induced by rosiglitazone did not reach statistical significance (Fig. 4H). Furthermore, HFD mice treated with a low dosage of the two compounds showed a similar trend but with no difference in bone trabecular morphometry (Fig. 4I and J). In addition, dynamic histomorphometry indicated that both HFD-Rosi and HFD-CMHX mice treated with 10 mg/kg/day showed significantly decreased MAR in trabecular bone compared with that of HFD-Veh and that a lower MAR was observed in HFD-Rosi mice than in HFD-CMHX mice (Fig. 4K).

Inhibition of osteoblast differentiation by CMHX008 was weaker than rosiglitazone

At day 7 of osteoblast differentiation, rosiglitazone treatment significantly downregulated the protein levels of OCN, and Runx2 protein showed decreased trend. However, CMHX008 treatment did not alter OCN and Runx2 protein levels (Fig. 5A). On day 14, the cells were stained for ALP (Fig. 5B), and the ALP activities (Fig. 5C) and mRNA levels of Ocn and Runx2 (Fig. 5D) were measured. Both rosiglitazone and CMHX008 treated cells displayed a reduced number of osteoblast compared with vehicle treatment. However, rosiglitazone treatment showed a more significant reduction in the number of osteoblast cells compared with that of CMHX008 treatment. These changes were correlated with decreased ALP activities (Fig. 5C) and reduced mRNA levels of expression of Ocn and Runx2 (Fig. 5D), suggesting that the capacity of bone formation was more robustly inhibited by rosiglitazone. Furthermore, on day 21, ARS, an indicator of calcium deposition, was performed to quantify osteoblast differentiation. Both rosiglitazone and CMHX008-treated cells produced significantly fewer mineralized matrix compared with vehicle-treated cells

(Fig. 5E). CMHX008 treatment displayed a more mineralized matrix than rosiglitazone treatment (Fig. 5E).

Discussion

Classical TZDs carry great concerns due to their increased risk of fluid retention, weight gain and bone loss, even though they are efficacious in the treatment of T2DM.⁶ PPAR γ partial agonists maintain the antidiabetic properties of TZDs but present minimal negative effects.^{20,21} The present study aimed to compare the insulin sensitizing effects and bone loss side effects of CMHX008 with those of the classical PPAR γ agonist, rosiglitazone. Recent studies provided direct evidence that CMHX008 binds to the LBD of PPAR γ with lower affinity than rosiglitazone via TR-FRET ligand-binding assay. Compared with a previous short-term (5 weeks) administration protocol,²³ the presented sub-chronic treatment (16 weeks) of CMHX008 displayed similar antidiabetic properties, as did rosiglitazone treatment based on the improved effects on metabolic and glucose homeostasis. Notably, CMHX008 caused a lower degree of weight gain and bone loss compared with that of rosiglitazone. Mechanically, inhibition of phosphorylation of PPAR γ at serine 273 and the regulation of osteoblast differentiation from mesenchymal stem cells, might account for the advantageous pharmacological profiles of CMHX008.

TR-FRET ligand-binding assay is a sensitive and reliable method widely used for the determination of the PPAR γ binding affinity.^{28–30} The current results showed that CMHX008 directly bound to PPAR γ -LBD with IC₅₀ and Ki values almost 3-fold higher than those of rosiglitazone did, indicating that CMHX008 exerted a lower binding affinity to PPAR γ . The binding affinity of CMHX008 was the same as those of the previously reported partial agonists GQ-16³¹ and amorfrutins¹⁷ but was weaker than that of honokiol²⁹ according to Ki values. Cell-based reporter assays showed that CMHX008 was a selective activator of PPAR γ without the activation of either PPAR α or PPAR δ .²³ Accordingly, recent data confirmed that CMHX008 was a selective PPAR γ ligand with weaker agonistic activity. The pharmacological profile may contribute to the recruitment of coactivators and may activate the transcriptional activity of PPAR γ in a weaker way than typical full agonist rosiglitazone does, which has been observed for other partial agonists.³⁰

Several natural or synthetic PPAR γ partial agonists retained similar antidiabetic effects as rosiglitazone but showed minimized side effects, such as weight gain.^{22,30,32–34} Consistent with these findings, CMHX008 showed a similar efficacy as rosiglitazone in ameliorating glucose homeostasis in HFD or *ob/ob* mice in the absence of weight gain. We also observed increased oxygen consumption and carbon dioxide production as measured by indirect calorimetry, suggesting that CMHX008, similar to other PPAR γ partial agonists, such as GQ-16, shared similar improving effects on the metabolic rate with rosiglitazone.³⁵ The comparable hypoglycemic effect and weaker agonistic behavior of the receptor between CMHX008 and rosiglitazone suggested a potential PPAR γ -independent mechanism. As the inhibition of PPAR γ phosphorylation at serine 273 by rosiglitazone is an important pharmacological

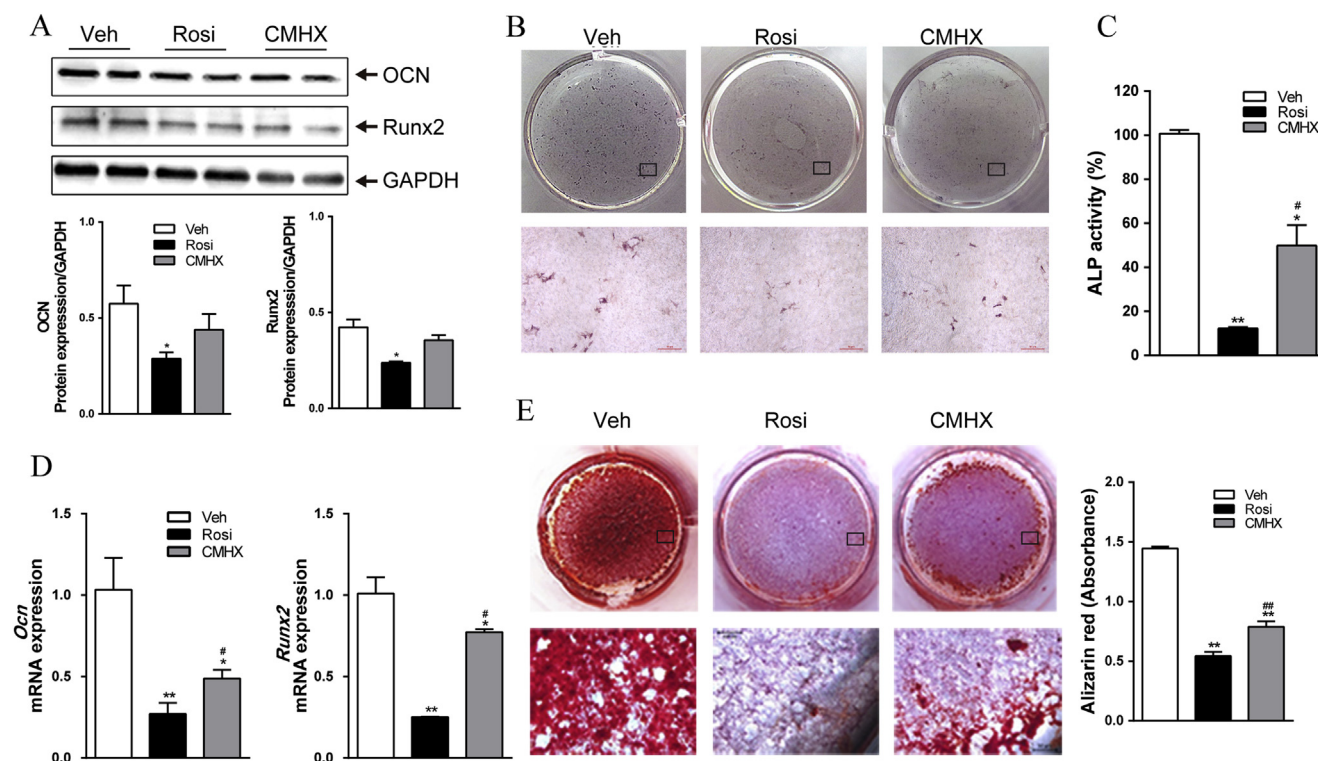


Figure 5 Effect of rosiglitazone (Rosi) or CMHX008 (CMHX) on the differentiation of mesenchymal stem cells (MSCs) into osteoblasts. (A) Protein levels of the osteogenic marker gene OCN and Runx2 in MSCs after treatment with vehicle (Veh), rosiglitazone (Rosi) or CMHX008 (CMHX) for 7 days. (B) Representative ALP staining of osteoblasts after treatment for 14 days. Scale bar = 50 μ m. (C) Quantitative ALP concentration after treatment for 14 days. (D) Expression of osteogenic marker genes by RT-PCR after treatment for 14 days. (E) Alizarin red staining of mineralized nodules after treatment for 21 days. * $P < 0.05$, ** $P < 0.01$ versus Veh, # $P < 0.05$, ## $P < 0.01$ versus Rosi.

feature¹⁹ that contributes to its anti-diabetic effects, we examined the changes in PPAR γ phosphorylation after CMHX008 treatment. Similar to the other natural or synthetic PPAR γ partial agonists, such as amorfrutins,¹⁷ cherythrine,²² F12016,³⁰ and dihydromyricetin,³⁶ CMHX008 induced the obvious inhibition of PPAR γ phosphorylation, suggesting that this compound exerts antidiabetic effects via the inhibition of PPAR γ phosphorylation, without activating the full range of PPAR γ targets, and thereby avoiding known side effects, such as weight gain.

Another negative effect of the long-term administration of rosiglitazone is the impairment of osteoblastogenesis, which leads to osteoporosis and an increased risk of bone fractures.^{9,10,37} The fact that ligands with lower agonistic effects on PPAR γ or even PPAR γ suppressors exhibit beneficial influences on skeleton homeostasis^{30,38–41} prompted us to determine the effect of CMHX008 on bone density and bone turnover parameters. The micro-CT-determined skeletal mass and parameters of trabecular bone architecture displayed a decreased number of trabecular bone in HFD and *ob/ob* mice, suggesting that obesity is one of the risk factors in inducing osteoporosis⁴² and rosiglitazone or CMHX008 administration displayed a further loss of trabecular bone. However, mice treated with rosiglitazone had more severe decline in bone density than did those treated with CMHX008, suggesting that CMHX008 will cause less osteoporosis compared with the PPAR γ agonist rosiglitazone. The activation of PPAR γ inhibited osteoblast

differentiation and promoted osteoclast differentiation, resulting in bone loss via the concerted inhibition of bone formation and stimulation of bone resorption.⁴³ In addition, osteoblasts and adipocytes share a common progenitor, MSCs, which are associated with a reciprocal decrease of osteogenesis and an increase of adipogenesis. Under conditions of osteoblast differentiation, MSCs treated with rosiglitazone exhibited more significant inhibition of calcium deposition and osteogenesis compared with CMHX008 treatment, which was consistent with the changes in osteogenic markers OCN, and Runx2 at mRNA and protein levels. Accordingly, dynamic histomorphometry showed that HFD-fed mice treated with rosiglitazone showed a significantly lower bone MAR and lower bone mass in trabecular bone than did CMHX008 treatment, suggesting that the capacity of bone formation was less considerably inhibited by CMHX008. The lower inhibition of osteoblastogenesis by CMHX008 observed in the current studies was also consistent with that of other PPAR γ partial agonists.^{30,38,41}

In conclusion, our present study provides new evidence of ligand-dependent regulation on adipogenesis and osteoblastogenesis through PPAR γ . CMHX008 displays a lower PPAR γ activity, attenuates the metabolic defects in obese mice, does not carry side effects of weight gain, and shows minor osteoporotic complications compared with rosiglitazone. These pharmacological profiles are correlated with the ability of this compound to block the

phosphorylation of PPAR γ at serine 273 and reduce the osteogenic properties of PPAR γ , which subsequently favors osteoblastogenesis over adipogenesis. Our study also suggests that these activities can be pharmacologically separated and individually harnessed by specifically designed selective PPAR γ agonists to retain insulin sensitization without the classical lipogenic and osteoporotic side effects.

Conflict of interest

The authors declare no conflict of interest.

Acknowledgment

This work was supported by the National Natural Science Foundation of China (81270947 and 81570763, to XX), the National Program on Key Basic Research Project of China (973 Program, 2012CB517505, to XX), the Fundamental Science and Advanced Technology Research of Chongqing (Major Project, CSTC2015jcyjB0146), and Chongqing Graduate Student Research Innovation Fund (CYB15095, to HY). We are grateful to Prof. Xiaochao Yang from School of Biomedical Engineering, the Third Military Medical University, for the critical comments on the manuscript.

References

1. Jaacks LM, Siegel KR, Gujral UP, Narayan KM. Type 2 diabetes: a 21st century epidemic. *Best Pract Res Clin Endocrinol Metab.* 2016;30(3):331–343.
2. Zimmet P, Alberti KG, Magliano DJ, Bennett PH. Diabetes mellitus statistics on prevalence and mortality: facts and fallacies. *Nat Rev Endocrinol.* 2016;12(10):616–622.
3. Spiegelman BM. PPAR-gamma: adipogenic regulator and thiazolidinedione receptor. *Diabetes.* 1998;47(4):507–514.
4. Kong AP, Yamasaki A, Ozaki R, et al. A randomized-controlled trial to investigate the effects of rivoglitazone, a novel PPAR gamma agonist on glucose-lipid control in type 2 diabetes. *Diabetes Obes Metab.* 2011;13(9):806–813.
5. Nissen SE, Wolski K. Effect of rosiglitazone on the risk of myocardial infarction and death from cardiovascular causes. *N Engl J Med.* 2007;356(24):2457–2471.
6. Hiatt WR, Kaul S, Smith RJ. The cardiovascular safety of diabetes drugs — insights from the rosiglitazone experience. *N Engl J Med.* 2013;369(14):1285–1287.
7. Consoli A, Formoso G. Do thiazolidinediones still have a role in treatment of type 2 diabetes mellitus? *Diabetes Obes Metab.* 2013;15(11):967–977.
8. Lecka-Czernik B. Diabetes, bone and glucose-lowering agents: basic biology. *Diabetologia.* 2017;60(7):1163–1169.
9. Billington EO, Grey A, Bolland MJ. The effect of thiazolidinediones on bone mineral density and bone turnover: systematic review and meta-analysis. *Diabetologia.* 2015;58(10):2238–2246.
10. Napoli N, Chandran M, Pierroz DD, Abrahamsen B, Schwartz AV, Ferrari SL. Mechanisms of diabetes mellitus-induced bone fragility. *Nat Rev Endocrinol.* 2017;13(4):208–219.
11. Watkins MP, Norris JY, Grimston SK, et al. Bisphosphonates improve trabecular bone mass and normalize cortical thickness in ovariectomized, osteoblast Connexin43 deficient mice. *Bone.* 2012;51(4):787–794.
12. Scotti E, Tontonoz P. Peroxisome proliferator-activated receptor gamma dances with different partners in macrophage and adipocytes. *Mol Cell Biol.* 2010;30(9):2076–2077.
13. Tontonoz P, Spiegelman BM. Fat and beyond: the diverse biology of PPARgamma. *Annu Rev Biochem.* 2008;77:289–312.
14. Cao J, Ou G, Yang N, et al. Impact of targeted PPARgamma disruption on bone remodeling. *Mol Cell Endocrinol.* 2015;410:27–34.
15. Cock TA, Houten SM, Auwerx J. Peroxisome proliferator-activated receptor-gamma: too much of a good thing causes harm. *EMBO Rep.* 2004;5(2):142–147.
16. Choi SS, Kim ES, Jung JE, et al. PPARgamma antagonist gleevec improves insulin sensitivity and promotes the browning of white adipose tissue. *Diabetes.* 2016;65(4):829–839.
17. Weidner C, de Groot JC, Prasad A, et al. Amorphutins are potent antidiabetic dietary natural products. *Proc Natl Acad Sci USA.* 2012;109(19):7257–7262.
18. Higgins LS, Depaoli AM. Selective peroxisome proliferator-activated receptor gamma (PPARgamma) modulation as a strategy for safer therapeutic PPARgamma activation. *Am J Clin Nutr.* 2010;91(1):267S–272S.
19. Choi JH, Banks AS, Estall JL, et al. Anti-diabetic drugs inhibit obesity-linked phosphorylation of PPARgamma by Cdk5. *Nature.* 2010;466(7305):451–456.
20. DePaoli AM, Higgins LS, Henry RR, Mantzoros C, Dunn FL. Can a selective PPARgamma modulator improve glycemic control in patients with type 2 diabetes with fewer side effects compared with pioglitazone? *Diabetes Care.* 2014;37(7):1918–1923.
21. Dunn FL, Higgins LS, Fredrickson J, DePaoli AM. Selective modulation of PPARgamma activity can lower plasma glucose without typical thiazolidinedione side-effects in patients with Type 2 diabetes. *J Diabet Complicat.* 2011;25(3):151–158.
22. Zheng W, Qiu L, Wang R, et al. Selective targeting of PPAR-gamma by the natural product chelerythrine with a unique binding mode and improved antidiabetic potency. *Sci Rep.* 2015;5:12222.
23. Ming Y, Hu X, Song Y, et al. CMHX008, a novel peroxisome proliferator-activated receptor gamma partial agonist, enhances insulin sensitivity in vitro and in vivo. *PLoS One.* 2014;9(7):e102102.
24. Song Y, Li J, Zhao Y, et al. Severe maternal hyperglycemia exacerbates the development of insulin resistance and fatty liver in the offspring on high fat diet. *Exp Diabetes Res.* 2012;2012:254976.
25. Liu Z, Lim CY, Su MY, et al. Neonatal overnutrition in mice exacerbates high-fat diet-induced metabolic perturbations. *J Endocrinol.* 2013;219(2):131–143.
26. Yuasa M, Yamada T, Taniyama T, et al. Dexamethasone enhances osteogenic differentiation of bone marrow- and muscle-derived stromal cells and augments ectopic bone formation induced by bone morphogenetic protein-2. *PLoS One.* 2015;10(2). e0116462.
27. Banks AS, McAllister FE, Camporez JP, et al. An ERK/Cdk5 axis controls the diabetogenic actions of PPARgamma. *Nature.* 2015;517(7534):391–395.
28. Stechschulte LA, Czernik PJ, Rotter ZC, et al. PPARG post-translational modifications regulate bone formation and bone resorption. *EBioMedicine.* 2016;10:174–184.
29. Atanasov AG, Wang JN, Gu SP, et al. Honokiol: a non-adipogenic PPAR γ agonist from nature. *Biochim Biophys Acta Gen Subj.* 2013;1830(10):4813–4819.
30. Liu C, Feng T, Zhu N, et al. Identification of a novel selective agonist of PPARgamma with no promotion of adipogenesis and less inhibition of osteoblastogenesis. *Sci Rep.* 2015;5:9530.
31. Amato AA, Rajagopalan S, Lin JZ, et al. GQ-16, a novel peroxisome proliferator-activated receptor gamma (PPAR-gamma) ligand, promotes insulin sensitization without weight gain. *J Biol Chem.* 2012;287(33):28169–28179.

32. Chen Z, Vigueira PA, Chambers KT, et al. Insulin resistance and metabolic derangements in obese mice are ameliorated by a novel peroxisome proliferator-activated receptor gamma-sparing thiazolidinedione. *J Biol Chem.* 2012;287(28):23537–23548.
33. Zhang X, Liu H, Sun B, et al. Novel podophyllotoxin derivatives as partial PPARgamma agonists and their effects on insulin resistance and type 2 diabetes. *Sci Rep.* 2016;6:37323.
34. Atanasov AG, Blunder M, Fakhrudin N, et al. Polyacetylenes from *Notopterygium incisum*—new selective partial agonists of peroxisome proliferator-activated receptor-gamma. *PLoS One.* 2013;8(4):e61755.
35. Coelho MS, de Lima CL, Royer C, et al. GQ-16, a TZD-derived partial PPARgamma agonist, induces the expression of thermogenesis-related genes in Brown fat and visceral white fat and decreases visceral adiposity in obese and hyperglycemic mice. *PLoS One.* 2016;11(5). e0154310.
36. Liu L, Wan J, Lang H, et al. Dihydromyricetin delays the onset of hyperglycemia and ameliorates insulin resistance without excessive weight gain in Zucker diabetic fatty rats. *Mol Cell Endocrinol.* 2017;439:105–115.
37. Schwartz AV, Chen H, Ambrosius WT, et al. Effects of TZD use and discontinuation on fracture rates in ACCORD bone study. *J Clin Endocrinol Metab.* 2015;100(11):4059–4066.
38. Kolli V, Stechschulte LA, Dowling AR, Rahman S, Czernik PJ, Lecka-Czernik B. Partial agonist, telmisartan, maintains PPARgamma serine 112 phosphorylation, and does not affect osteoblast differentiation and bone mass. *PLoS One.* 2014;9(5):e96323.
39. Marciano DP, Kuruville DS, Boregowda SV, et al. Pharmacological repression of PPAR γ promotes osteogenesis. *Nat Commun.* 2015;6:7443.
40. Silva JC, Cesar FA, de Oliveira EM, et al. New PPARgamma partial agonist improves obesity-induced metabolic alterations and atherosclerosis in LDLr(-/-) mice. *Pharmacol Res.* 2016;104:49–60.
41. Fukunaga T, Zou W, Rohatgi N, Colca JR, Teitelbaum SL. An insulin-sensitizing thiazolidinedione, which minimally activates PPAR γ , does not cause bone loss. *J Bone Miner Res.* 2015;30(3):481–488.
42. Neglia C, Argentiero A, Chitano G, et al. Diabetes and obesity as independent risk factors for osteoporosis: updated results from the ROIS/EMEROS registry in a population of five thousand post-menopausal women living in a region characterized by heavy environmental pressure. *Int J Environ Res Publ Health.* 2016;13(11).
43. Wan Y. PPAR γ in bone homeostasis. *Trends Endocrinol Metab.* 2010;21(12):722–728.